Theoretical and Computational Acoustics
D. Lee, Y-H Pao, M.H. Schultz, and Y-C Teng (Editors)
© 1996 World Scientific Publishing Co.

A Formulation in the Time Domain for the Acoustic Waveform Inversion: Synthetic Examples

G. Chavent
INRIA-Rocquencourt, Domaine de Voluceau, B.P. 105, F-78153 Le Chesnay Cédex
CEREMADE, Université de Paris 9, pl. du M[al] De Lattre De Tassigny,
F-75775 Paris Cédex 16

F. Clément
INRIA-Rocquencourt, Domaine de Voluceau, B.P. 105, F-78153 Le Chesnay Cédex

S. Gómez
IIMAS, National University of Mexico, Apdo. Postal 20-726, Mexico D.F.

B. Lavaud
INRIA-Rocquencourt, Domaine de Voluceau, B.P. 105, F-78153 Le Chesnay Cédex

Abstract

This work addresses the automatic determination of background slownesses in 2D structures from common shot full waveform acoustic data. When set as a least-squares minimization problem controlled by the background slowness and the reflectivity in the depth domain, the inversion problem shows two difficulties: (1) for fixed reflectivity in the depth domain, phase shifts are responsible for the presence of many local minima for the least-squares criterion, and (2) for wrong background slowness, when the structure to be imaged is complex, destructive interferences are responsible for the flatness of the criterion. The Migration-Based TravelTime (MBTT) formulation cures the phase shift problem by introducing a reflectivity unknown in the time domain. It is related to the reflectivity in the depth domain through a migration step which depends on the current background slowness. In the case of complex structures, time continuation has the benefit effect of widening the valley of the global minimum. This helps local minimization methods to reach the global minimum from rather poor initial guesses. We give numerical results of the inversion of synthetic models with simple and complex structure.

1 Introduction

Given a forward acoustic modeling, one can associate to any slowness ν and impedance σ the corresponding collection of synthetic seismograms for all shots,

$$(\nu, \sigma) \longmapsto c = (c_1, \ldots, c_N), \tag{1}$$

by sampling at the surface along the time the solution of the forward modeling. Then, one can set the geophysical problem of the determination of the Earth material properties ν and σ in 2D structures from a collection of surface seismic data $d = (d_1, \ldots, d_N)$ as an inverse problem through the minimization of the least-squares data misfit function

$$\mathcal{J} = \sum_{n=1}^{N} \mathcal{J}_n \qquad \text{with} \qquad \mathcal{J}_n = \frac{1}{2}\|d_n - c_n\|^2, \tag{2}$$

where $||.||$ is the Euclidean norm on the space of seismograms.

The difficulty is that the criterion $\mathcal{J}$ is highly non convex with respect to the longest wavelengths of the slowness unknown. This prevents local optimization methods to find the global minimum, and moreover, due to the huge amount of data and unknowns to handle, global optimization methods are far too expensive.

Focusing on local methods, we decided to modify the objective function by introducing a new reflectivity unknown in the time domain: this is the Migration-Based TravelTime (MBTT) reformulation, *cf.* [7, 4, 3, 5], which cures the phase shift problem. This approach is related to works by Chavent and Jacewitz, *cf.* [6],and Symes *et al.*, *cf.* [11, 12]. In order to deal with complex structures, we have to overcome the destructive interferences problem, and we propose to widen the valley of the global minimum of the criterion by using time continuation.

After introducing propagator and reflector unknowns which are more suited for the representation of the physical phenomena, we construct a quantitative migration operator which is aimed at restoring the true amplitudes of the reflectors. Then the MBTT formulation consists in a change of reflector unknown through a quantitative migration step. We propose a minimization strategy based on the time continuation principle and we give numerical results of the inversion of noise free synthetic data sets (described in Appendix).

2 The least-squares criterion

We consider here a forward modeling computed through a finite differences discretization of the full 2D acoustic wave equation. A multiscale analysis, *cf.* [8, 4], shows that one can associate long wavelengths of the slowness to the propagation of energy, short wavelengths of both the slowness and the impedance to the reflection of energy and long wavelengths of the impedance to smaller effects.

Let us denote by V the discrete space for the material properties ν and σ. We consider an orthogonal decomposition of this space into the direct sum $V = V_s \oplus V_r$, where V_s is a space of "smooth" or slowly varying functions and V_r is a space of "rough" or rapidly oscillating functions, *cf.* [4] for an example of such a decomposition. Then we define a "propagator" unknown π and a "reflector" unknown r by setting

$$\pi = \nu_s \qquad \text{and} \qquad r = (\nu_r, \sigma_r) \tag{3}$$

where the $_s$ and $_r$ subscripts stand respectively for the projections on the subspaces V_s and V_r. The smooth projection of the impedance is supposed constant.

Let $\Pi = V_s$ be the space of propagators, $R = V_r \times V_r$ be the space of reflectors and D be the space of seismograms. We denote by φ the forward modeling,

$$\begin{array}{rccl} \varphi: & \Pi \times R & \longrightarrow & D \\ & (\pi, r) & \longmapsto & c = (c_1, \ldots, c_N) \end{array} \tag{4}$$

and we set the waveform inversion problem as

(P) minimize $\mathcal{J}$ with respect to $\pi \in \Pi$ and $r \in R$,

where the least-squares criterion is defined by (2).

For fixed propagator $\pi \in \Pi$, the problem (P) presents no difficulty: $\mathcal{J}$ is almost quadratic with respect to the reflector r, and moreover, its Hessian $\nabla^2_{rr}\mathcal{J}$ is almost diagonal, *cf.* [10]. Thus, gradient-based methods give very good results, *cf.* section 3.

For fixed reflector $r \in R$, the problem (P) is very difficult: $\mathcal{J}$ is highly non convex with respect to the propagator π. There are two main reasons for this non convexity: (1) the phase shift problem, which is responsible for the presence of local minima, and (2) the destructive interferences problem, which is responsible for the flatness of the criterion far from the global minimum. Notice that the latter is only significant for media with complex structures. The time formulation, *cf.* section 4, cures the phase shift problem and it is necessary to widen the attraction domain of the global minimum when dealing with complex structures.

3 Quantitative migration

For any propagator $\pi \in \Pi$, let $B(\pi)$ be the linearized forward modeling operator,

$$B(\pi) = \frac{\partial \varphi}{\partial r}(\pi, 0). \tag{5}$$

It is well known, *cf.* [9, 13], that its transposed $B(\pi)^T$ is a migration operator: applied to the data $d = (d_1, \ldots, d_N) \in D$, it produces an image in the reflector space

$$m = B(\pi)^T d = -\nabla_r \mathcal{J} \in R. \tag{6}$$

This image is the stack of the migrated sections of each shot obtained by using propagator π, and it is also the local steepest descent direction for the criterion $\mathcal{J}$. But, because of the attenuation affecting the fields involved in the computation of the migrated sections, the amplitudes of the migrated events decay very rapidly with depth, and $B(\pi)^T$ restores only the location of the reflectors but not their amplitude.

A quantitative migration operator, *cf.* [3], has the additional property of also restoring the amplitude of the reflectors. We propose to construct such an operator by modifying the previous descent direction through

$$\mathcal{M}(\pi) = \Lambda B(\pi)^T. \tag{7}$$

The Newton minimization algorithm would suggest to use, as the preconditionning operator Λ, the inverse of the Hessian of the criterion $\mathcal{J}$. Although this Hessian is computationally out of reach and non invertible, it is also almost diagonal, *cf.* [10], and this leads us to take Λ in the class of positive diagonal matrices.

In this work, we choose a preconditionning proportional to the depth,

$$\Lambda = \lambda^\star \mathrm{diag}(z), \tag{8}$$

where the real number $\lambda^\star$ is the optimal step in the modified descent direction for the criterion $\mathcal{J}$ for some initial guess of the propagator π^0, *i.e.*

$$\lambda^\star = \arg\min_\lambda \mathcal{J}(\pi^0, \lambda \mathrm{diag}(z) B(\pi^0)^T d). \tag{9}$$

4 Formulation in the time domain

The Migration-Based TravelTime (MBTT) concept consists in replacing the search for the reflector in the depth domain $r \in R$ by the search for its dual variable, *cf.* [2], a reflectivity in the time domain $s = (s_1, \ldots, s_N) \in D$ where, for each propagator $\pi \in \Pi$,

$$r = \mathcal{M}(\pi)s \tag{10}$$

with the quantitative migration operator $\mathcal{M}(\pi)$ defined by (7), (8) and (9).

The new forward modeling operator,

$$\begin{array}{ccccc} \Pi \times D & \stackrel{\mathcal{M}(\pi)}{\longrightarrow} & \Pi \times R & \stackrel{\varphi}{\longrightarrow} & D \\ (\pi, s) & \longmapsto & (\pi, r) & \longmapsto & c, \end{array} \tag{11}$$

is called "resimulation" and it provides a revisited formulation of the waveform inversion as

(MP) minimize $\mathcal{J}$ with respect to $\pi \in \Pi$ and $s \in D$,

where $\mathcal{J}$ is the same least-squares criterion defined by (2).

We have shown in [5] that this change of reflectivity unknown does not lead to underparametrization and that it cures the phase shift problem: for reflectivity fixed in the time domain $s \in D$, changes in the propagator $\pi \in \Pi$ produce modifications of the reflector estimated in the depth domain $r \in R$ such that they annihilate the phase shifts that would have occured in the synthetics after simulation. This is illustrated in Figures 5 and 7 where, for a wrong propagator, each event in the resimulated seismograms is located at the correct time, but possibly with a wrong amplitude.

The second benefit of this time formulation is that, since $\mathcal{M}(\pi)$ is a quantitative migration operator, the data d is a good initial guess for the time reflectivity s. This is illustrated in Figures 3 and 4 where the resimulated seismograms are very close to the data.

5 Inversion results

All the optimizations performed here use a BFGS method with limited memory cost.

In the case of simple structures, the criterion $\mathcal{J}$ is only subject to the phase shift problem: notice how in Figure 5, where the propagator is constant, we can still identify the four reflectors of the SYNCLAY model. We propose then an alternate minimization strategy: first minimize $\mathcal{J}$ with respect to $\pi \in \Pi$ from an initial guess π^0 with $s^0 = d$ and obtain π^1, then minimize $\mathcal{J}$ with respect to $s \in D$ from s^0 with π^1 and obtain s^1, and so on... We show in [5] that a multiscaled representation of the propagator allows a hierarchical minimization which enhances the optimization, and that it is not necessary to repeat the alternate process. Figure 6 shows the result of this alternate minimization in the case of the SYNCLAY data, *cf.* Appendix. Although the initial propagator is very poor, $\pi^0 = 1/2500$ s/m, *cf.* Figure 5, the optimal propagator presents correct values in the illuminated areas, the estimated reflectors are correctly located and the amplitudes in the resimulated seismograms are also correctly restored (the criterion has decreased by a factor of 6).

In the case of complex structures, the criterion $\mathcal{J}$ is also subject to the destructive interferences problem: see how poor is the reflector estimated in the depth domain with a ramp propagator in Figure 7. Indeed, when applying exactly the same procedure as before to the

MARMOUSI data, *cf.* Appendix, even with a better initial propagator π^0 (a ramp rather a constant), we converge towards a local minimum which is far from the true propagator, *cf.* Figure 8. So, we propose to help the minimization process by widening the valley of the global minimum of the criterion $\mathcal{J}$ by increasing the number of shots (10 in stead of 5) and by performing time continuation. We define an increasing sequence $0 < T_1 < \ldots < T_p$ where T_p is the total duration of recording and for each $i = 1, \ldots, p$, $\mathcal{J}^i$ is the restriction of the least-squares data misfit function to the interval of time $[0, T_i]$. Then the minimization strategy is a generalization of the previous one: π^0 is given and $s^0 = d$, for $i = 1$ to p, minimize $\mathcal{J}^i$ with respect to π from π^{i-1} with s^{i-1} and obtain π^i, then minimize $\mathcal{J}^i$ with respect to s from s^{i-1} with π^i and obtain s^i. We show in Figure 9 the result of this "time progressive" alternate minimization in the case of the MARMOUSI data. The increasing sequence is 0.5 s, 0.7 s and 1 s. The optimal propagator and the estimated reflectors are almost correct in the upper half of the domain but there are still problems with the deeper part (the criterion has only decreased by a factor of 1.6).

6 Conclusion

When setting the seismic waveform inversion as a minimization problem controlled by the background slowness and by the reflectivity depth section, the difficulty is the non convexity of the least-squares criterion with respect to the background slowness.

The Migration-Based TravelTime (MBTT) formulation, by introducing a reflectivity in the time domain, solves the phase shift problem, which is the main reason for the non convexity in the case of models with simple structure. Thus, the MBTT change of reflectivity unknown allows the construction of a data misfit function which is amenable to minimization by local techniques and we have successfully inverted the SYNCLAY data set, using a very poor initial guess of the slowness.

In the case of complex structures, we also have to deal with the second main reason for the non convexity, the destructive interferences problem. The use of time continuation helps in widening the attraction domain of the global minimum and we have obtained encouraging partial results for the MARMOUSI data set.

Acknowledgment

This research was carried out as part of the Prestack Structural Interpretation consortium project (PSI) and part of the computational results were obtained on a Cray C98 at the Institut du Développement et des Resources en Informatique Scientifique. The authors hereby acknowledge the support provided by the sponsors of the PSI project and by IDRIS.

References

[1] A. Bourgeois, M. Bourget, P. Lailly, M. Poulet, P. Ricarte, and R. Versteeg. Marmousi, model and data. In R. Versteeg and G. Grau, editors, *The Marmousi Experience: workshop on Practical Aspects of Seismic Data Inversion*, Zeist, The Netherlands, 1991. Eur. Assoc. Expl. Geophys.

[2] G. Chavent. Duality methods for waveform inversion. *submitted to Geophysical Journal International*, 1995.

[3] G. Chavent and F. Clément. Quantitative migrations and resimulation techniques for waveform inversion via a Migration-Based TravelTime formulation. *submitted to Geophysics, previously released as Technical Report 1839, INRIA, Le Chesnay, France*, 1993.

[4] G. Chavent and F. Clément. Separating propagation and reflection parameters in the acoustic wave equation. *submitted to Geophysics, previously released as Technical Report 1839, INRIA, Le Chesnay, France*, 1993.

[5] G. Chavent, F. Clément, and S. Gómez. Migration-Based TravelTime inversion of 2D simple structures: the Synclay model. *submitted to Geophysics*, 1995.

[6] G. Chavent and C. A. Jacewitz. Automatic determination of background velocities by multiple migration fitting. *Geophysics*, 60(2), 1995.

[7] F. Clément. A migration-based travel-time formulation for the inversion of 2D seismic reflection data. In G. Cohen, L. Halpern, and P. Joly, editors, *Proc. of the 1st Internat. Conf. on Mathematical and Numerical Aspects of Wave Propagation Phenomena*, pages 455–461. INRIA and SIAM, SIAM, 1991.

[8] M. Jannane, W. Beydoun, E. Crase, D. Cao, Z. Koren, E. Landa, M. Mendes, A. Pica, M. Noble, G. Roeth, S. Singh, R. Sneider, A. Tarantola, D. Trezeguet, and M. Xie. Wavelength of earth structures that can be resolved from seismic reflection data. *Geophysics*, 54(7):906–910, july 1989. Short Note.

[9] P. Lailly. The seismic inverse problem as a sequence of before stack migrations. In *Proc. of the Conf. on Inverse Scattering, Theory and Applications*. SIAM, 1983.

[10] R.-E. Plessix, Y.-H. De Roeck, and G. Chavent. Automatic and simultaneous migration velocity analysis and waveform inversion of real data using MBTT/WKBJ formulation. In *Proc. of the 65th S.E.G. Annual Meeting*. Soc. of Expl. Geophys., 1995. Expanded abstracts.

[11] W. W. Symes and J. J. Carrazone. Velocity inversion by differential semblance optimization. *Geophysics*, 56(5), may 1991.

[12] W. W. Symes and M. Kern. Inversion of reflection seismograms by differential semblance analysis: algorithm structure and synthetic example. *Geophysical Prospecting*, 42(6):565–614, 1992.

[13] A. Tarantola. Linearized inversion of seismic reflection data. *Geophysical Prospecting*, 32:998–1015, 1984.

A Synthetic models

We describe here our two synthetic acoustic models. One has a simple structure, but with lateral variations, and the other has a very complex structure. In both cases, the medium is a 1 km $\times$ 1 km square with a resolution of 5 m, the velocity ranges from 1500 m/s to 4000 m/s, the density is constant of value $\bar{\rho} = 1000$ kg/m^3, the source is a Gaussian with peak frequency of 25 Hz, there are 49 hydrophones all over the medium, the recording duration is of 1 s, amplitudes are corrected by a factor $\sqrt{t}$ and the direct arrivals are muted off. Propagation is computed through a finite differences full acoustic simulator.

The simple model is the SYNCLAY model, *cf.* [4], it is made of 5 homogeneous layers. We show in Figure 1 (top) the smooth/rough decomposition of the slowness $(\bar{\nu}_s, \bar{\nu}_r)$, *cf.* section 2. We consider 5 shots located at 100 m, 300 m,..., 900 m and we show in Figure 1 (bottom) the corresponding seismograms, $(\bar{\nu} = \bar{\nu}_s + \bar{\nu}_r, \bar{\sigma} = \bar{\rho}/\bar{\nu}) \longmapsto d = (d_1, \ldots, d_5)$.

The complex model is extracted from the MARMOUSI model, *cf.* [1], it corresponds to the rectangle $[5800, 7400] \times [1160, 2600]$ (in m). In this paper, we still denote by MARMOUSI this "sub-MARMOUSI" model. We show in Figure 2 (top) the smooth/rough decomposition of the slowness $(\bar{\nu}_s, \bar{\nu}_r)$. We consider either the same 5 shots as before or 10 shots located at 50 m, 150 m,..., 950 m and we show in Figure 2 (middle, bottom) the corresponding seismograms, $(\bar{\nu} = \bar{\nu}_s + \bar{\nu}_r, \bar{\sigma} = \bar{\rho}/\bar{\nu}) \longmapsto d = (d_1, \ldots, d_{10})$.

In both cases, we will take the smooth impedance constant, $\sigma_s = 1.5\ 10^6$ kg/m^{2}s.

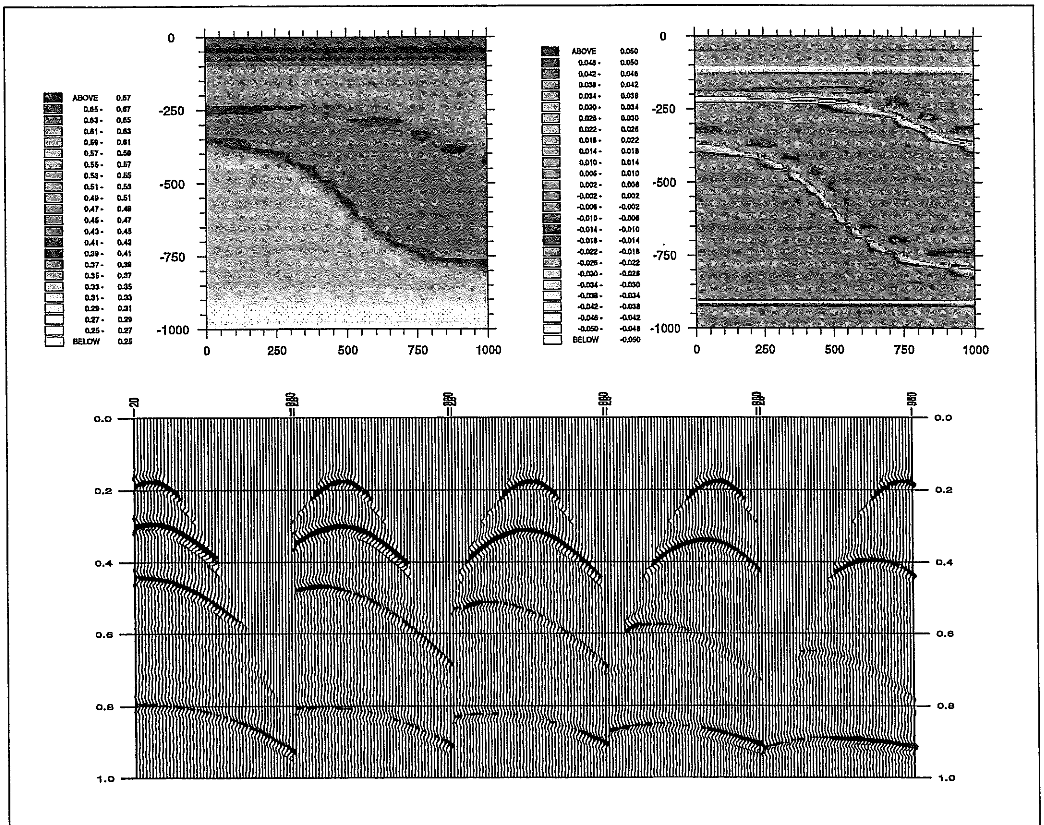

Figure 1: SYNCLAY model. Top: slowness (in 10^{-3} m/s), left: smooth slowness $\bar{\nu}_s$, sampled at $\simeq$ 50 m, right: rough slowness $\bar{\nu}_r$, sampled at $\simeq$ 5 m. Bottom: 5-shots data set.

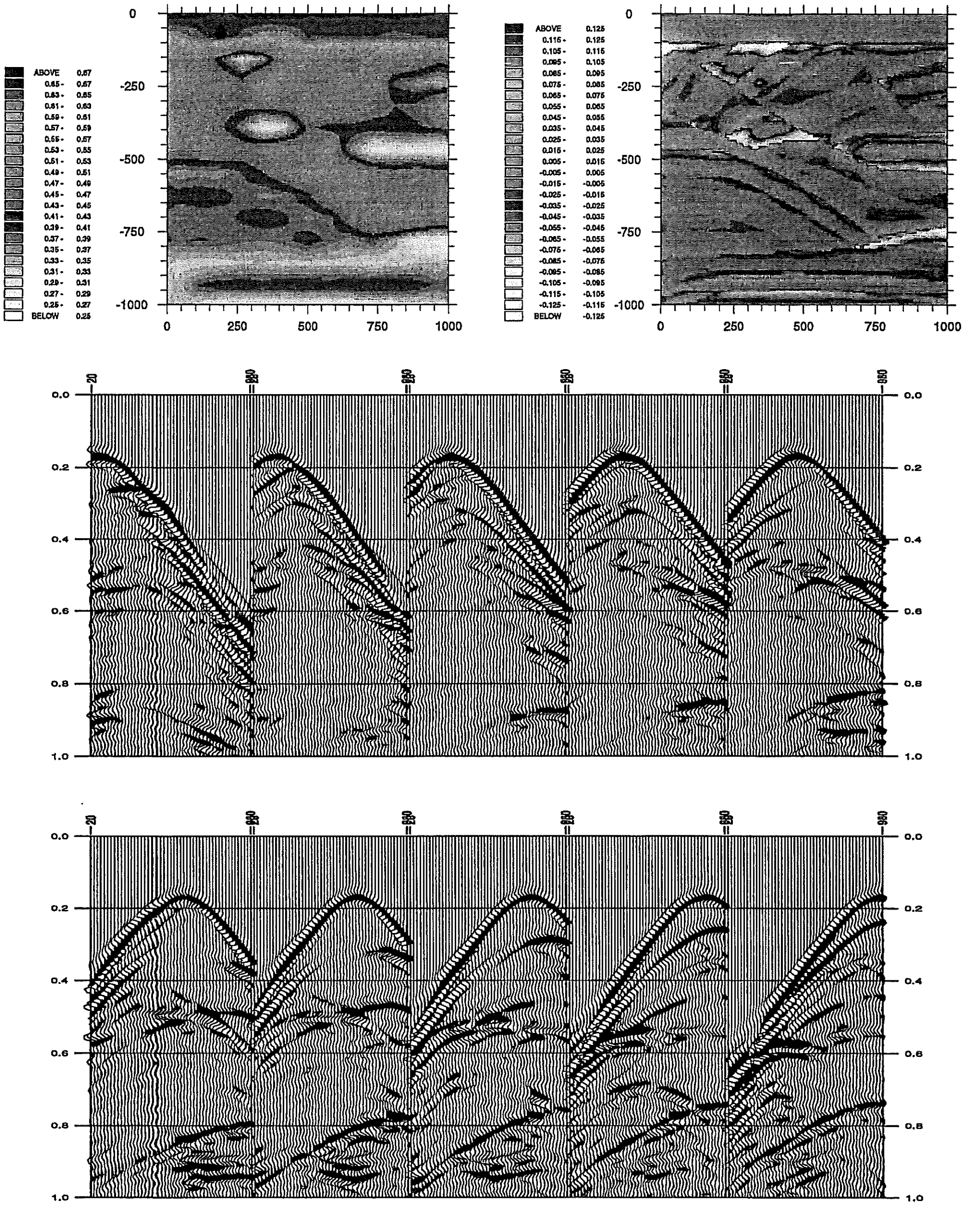

Figure 2: MARMOUSI model. Top: slowness (in 10^{-3} m/s), left: smooth slowness $\bar{\nu}_s$, sampled at $\simeq$ 50 m, right: rough slowness $\bar{\nu}_r$, sampled at $\simeq$ 5 m. Then 10-shots data set, middle: shots 1 to 5, bottom: shots 6 to 10.

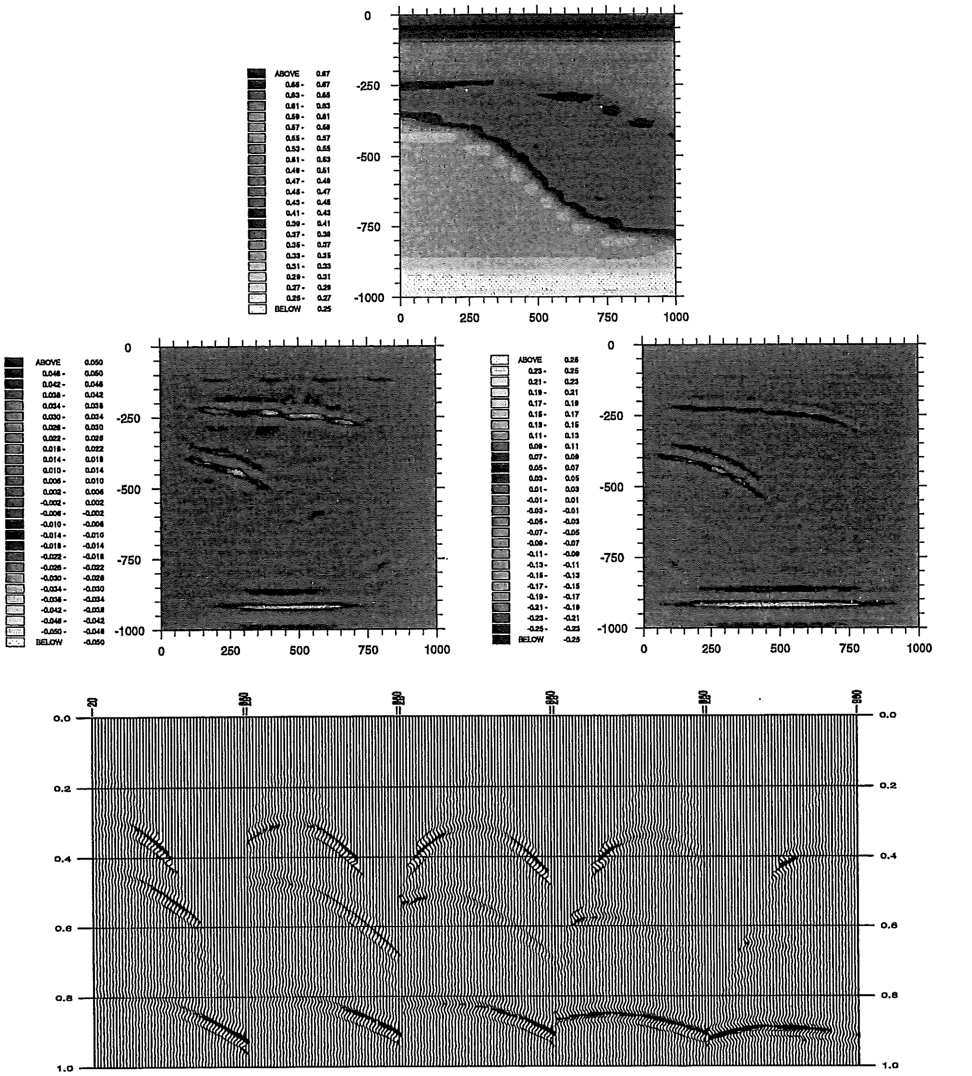

Figure 3: SYNCLAY model. Resimulation of the data $s^0 = d$ of Figure 1 with the true propagator. Top: true propagator $\bar{\pi}$. Middle: estimated reflectors r_ν (left) and r_σ (right). Bottom: simulation with propagator $\bar{\pi}$ and reflector $r = (r_\nu, r_\sigma)$.

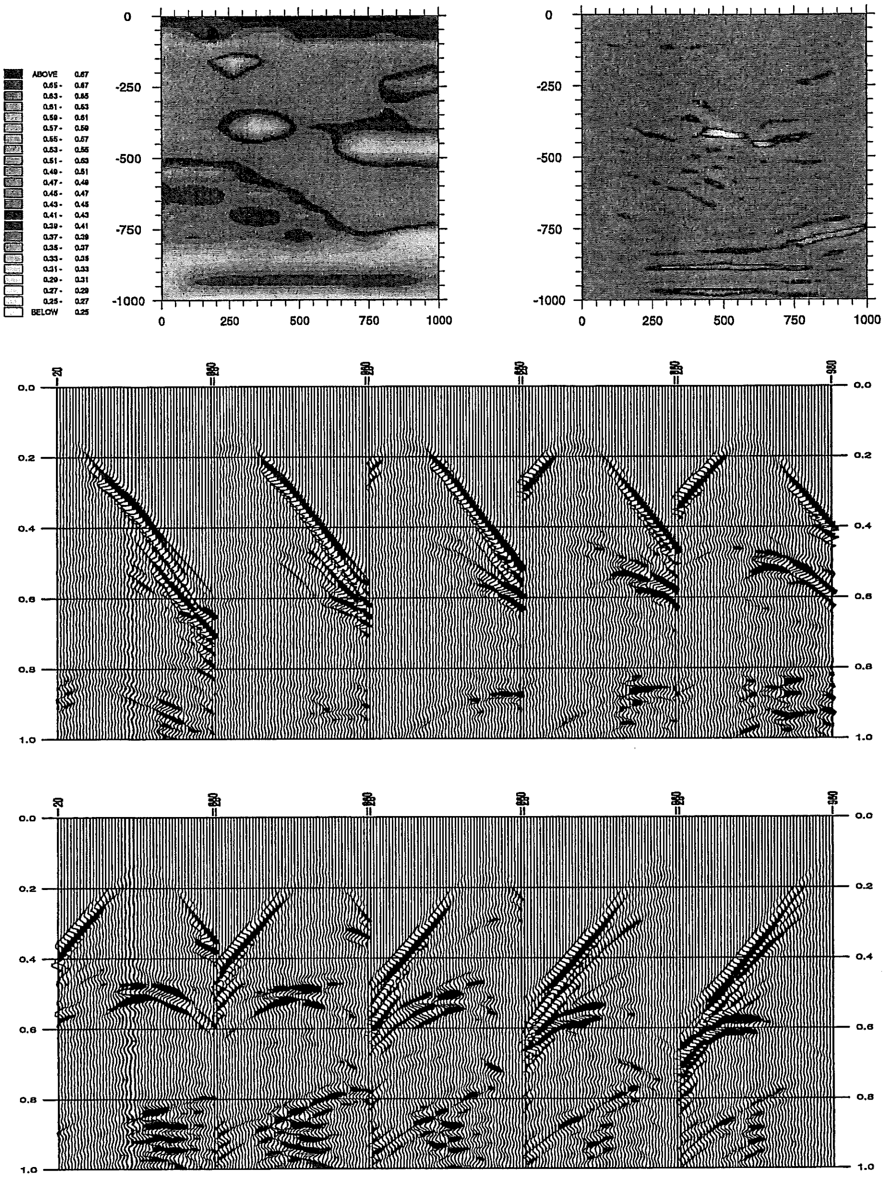

Figure 4: MARMOUSI model. Resimulation of the data $s^0 = d$ of Figure 2 with the true propagator. Top left: true propagator $\bar{\pi}$. Top right: estimated reflector r_σ. Then simulation with propagator $\bar{\pi}$ and reflector $r = (r_\nu, r_\sigma)$, middle: shots 1 to 5, bottom: shots 6 to 10.

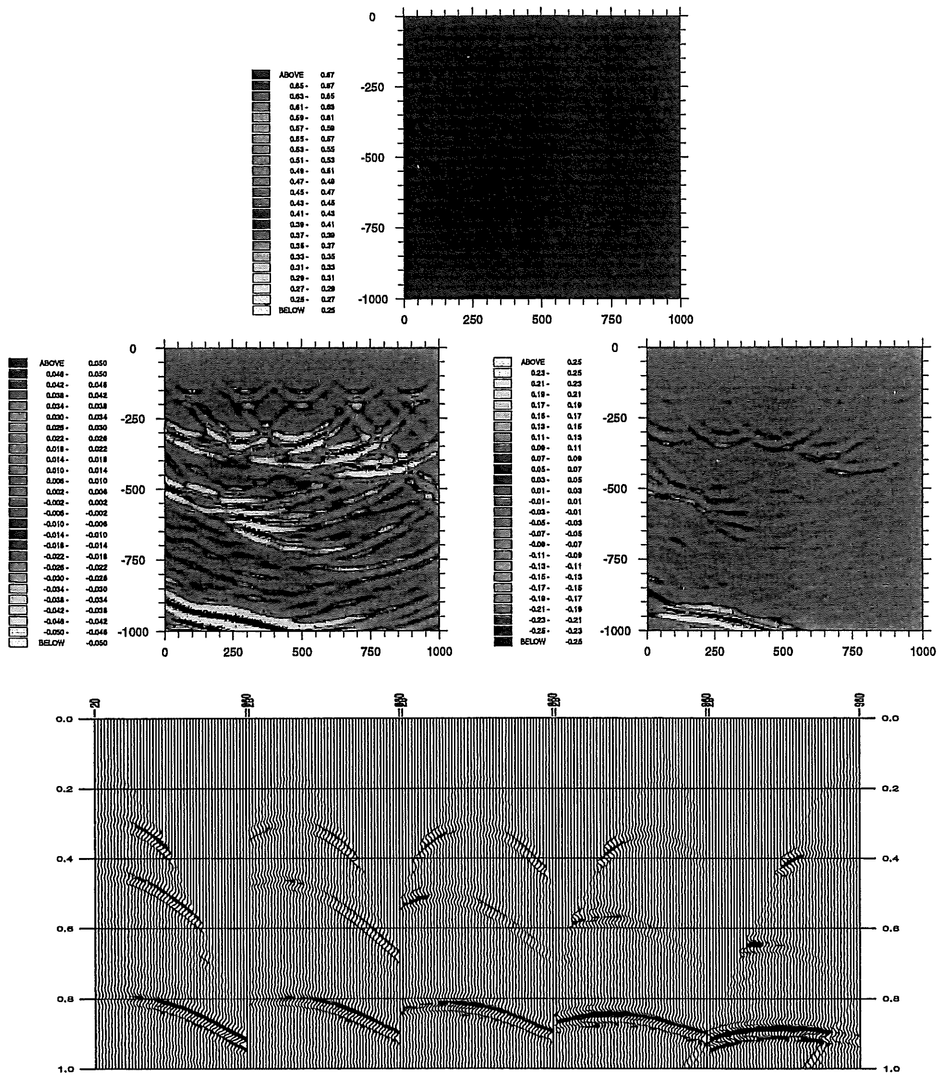

Figure 5: SYNCLAY model. Resimulation of the data $s^0 = d$ of Figure 1 with a constant propagator. Top: constant propagator $\pi^0 = 1/2500$ s/m. Middle: estimated reflectors r_ν (left) and r_σ (right). Bottom: simulation with propagator π^0 and reflector $r = (r_\nu, r_\sigma)$.

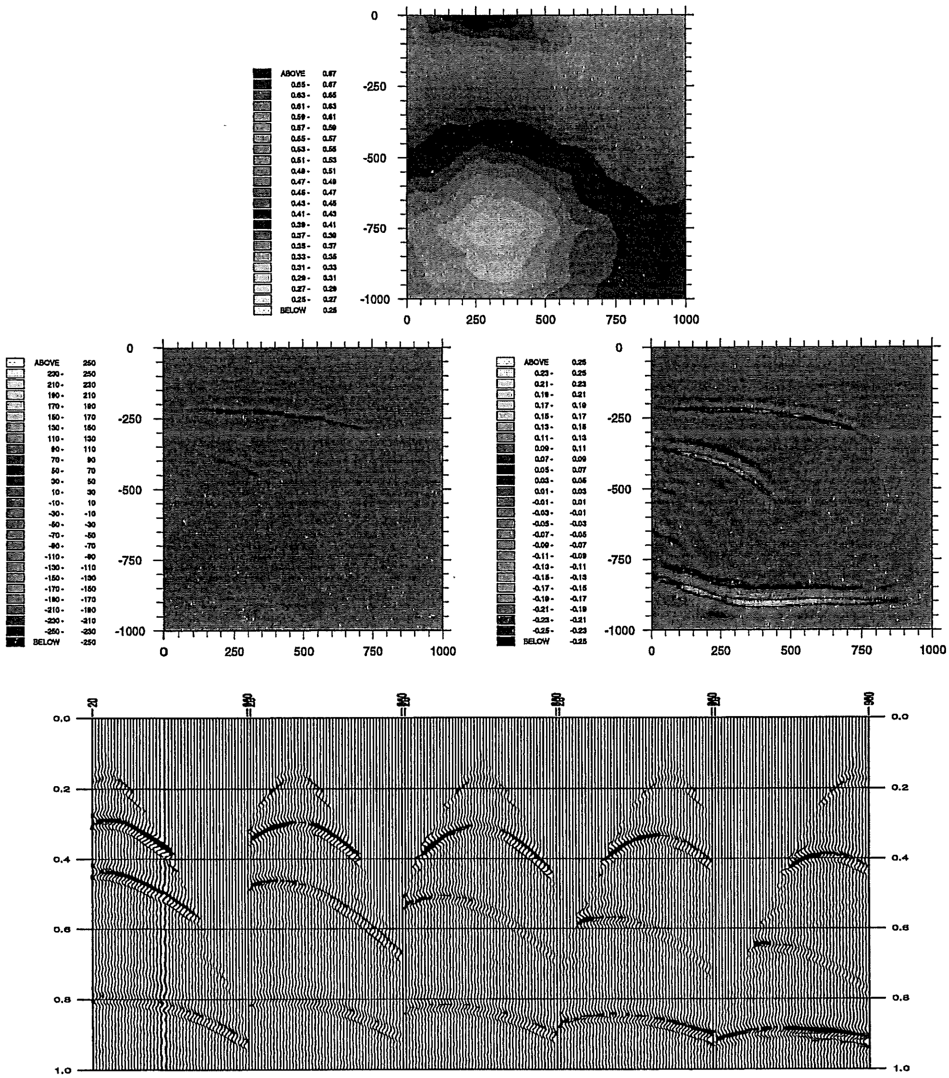

Figure 6: SYNCLAY model. Resimulation after alternate minimization. Top: optimal propagator $\pi^{\star}$. Middle: estimated reflectors r_{ν} (left) and r_{σ} (right). Bottom: simulation with propagator $\pi^{\star}$ and reflector $r = (r_{\nu}, r_{\sigma})$.

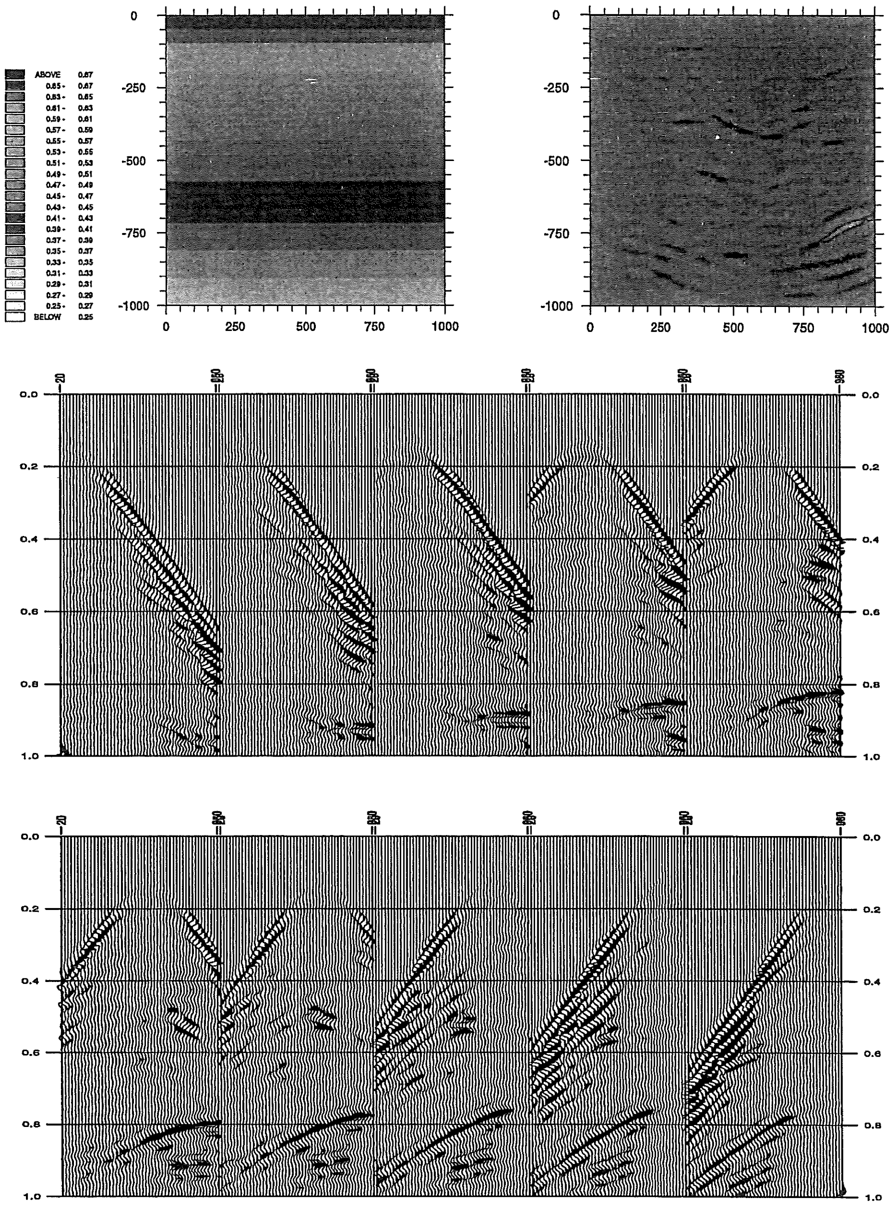

Figure 7: MARMOUSI model. Resimulation of the data $s^0 = d$ of Figure 2 with a ramp propagator. Top left: ramp propagator $\pi^0 = 1/1500\,\mathrm{s/m} - 1/3000\,\mathrm{s/m}$. Top right: estimated reflector r_σ. Then simulation with propagator π^0 and reflector $r = (r_\nu, r_\sigma)$, middle: shots 1 to 5, bottom: shots 6 to 10.

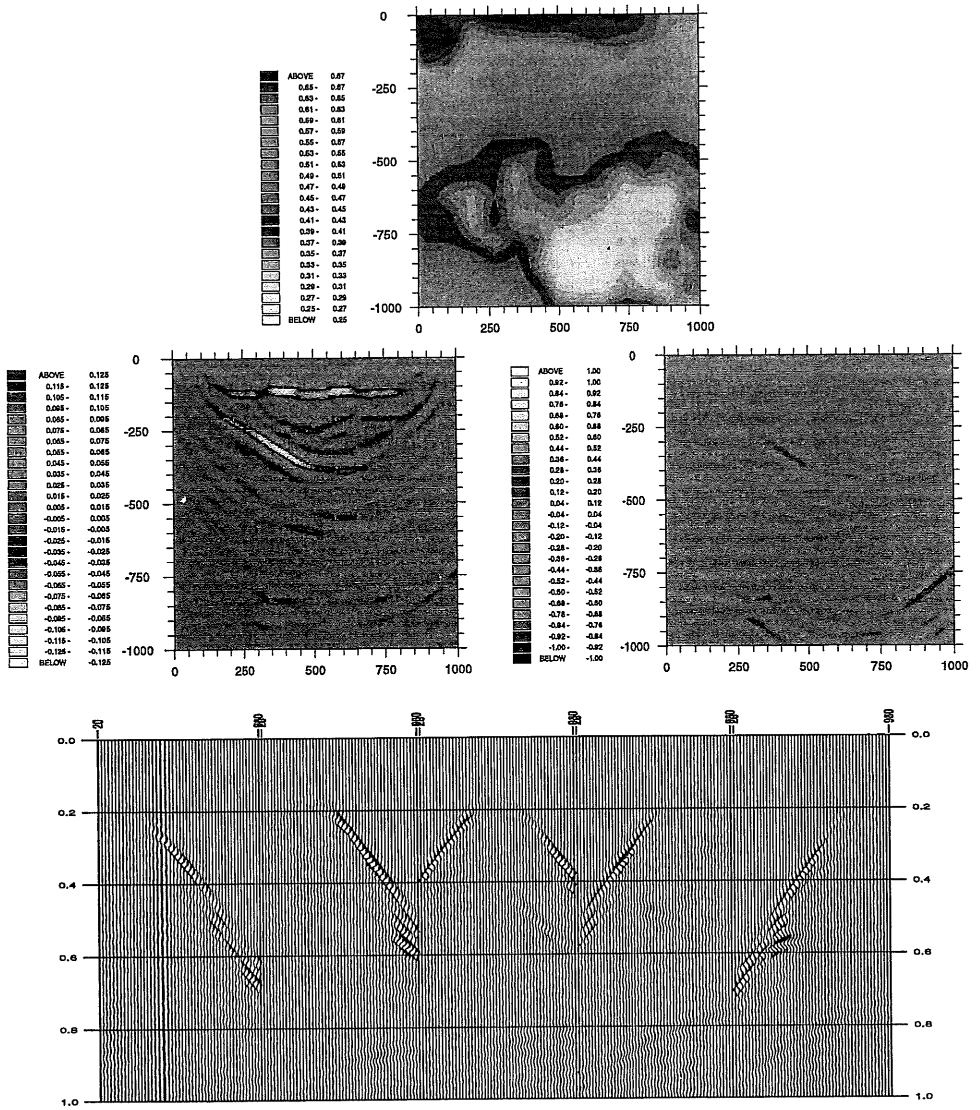

Figure 8: MARMOUSI model. Resimulation after alternate minimization. Top: optimal propagator $\pi^{\star}$. Middle: estimated reflectors r_{ν} (left) and r_{σ} (right). Bottom: simulation with propagator $\pi^{\star}$ and reflector $r = (r_{\nu}, r_{\sigma})$.

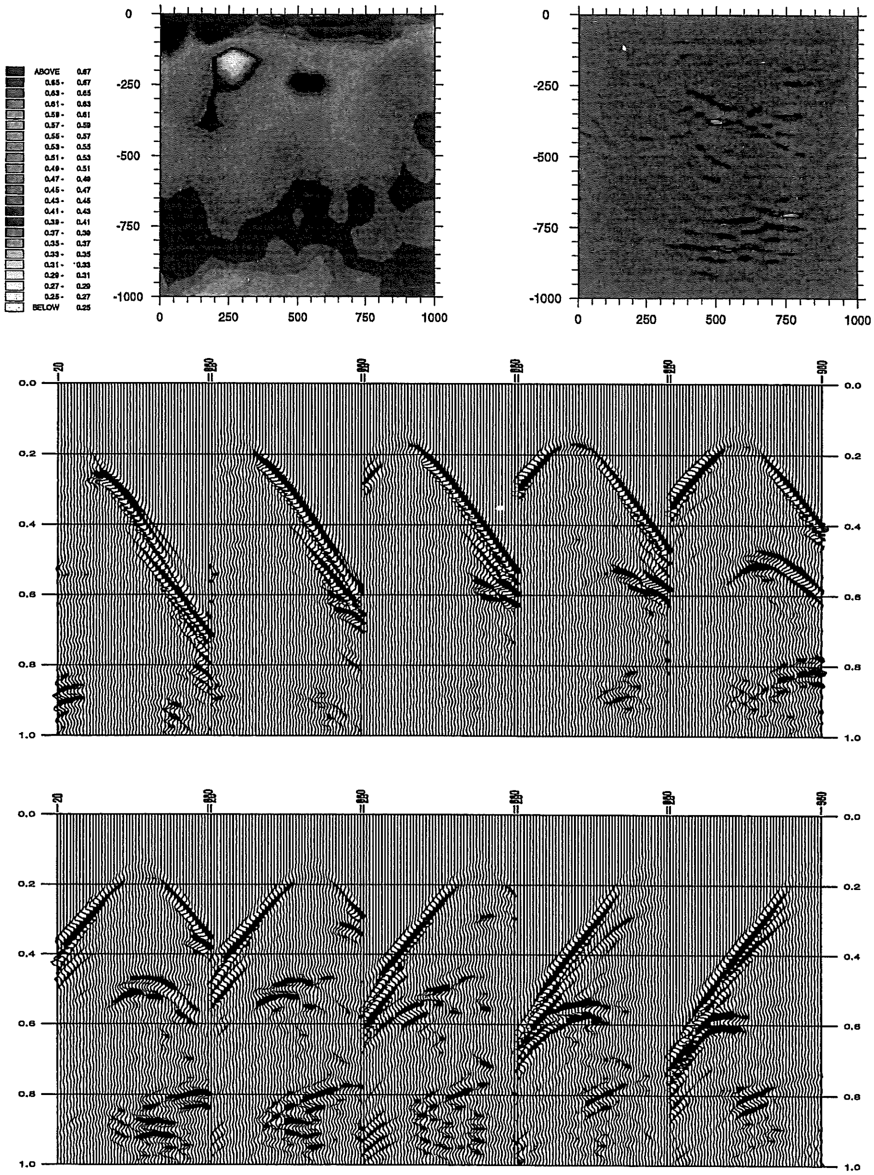

Figure 9: MARMOUSI model. Resimulation after "time progressive" alternate minimization. Top left: optimal propagator $\pi^{\star}$. Top right: estimated reflector r_{σ}. Then simulation with propagator $\pi^{\star}$ and reflector $r = (r_{\nu}, r_{\sigma})$, middle: shots 1 to 5, bottom: shots 6 to 10.